Multiple dimensionalities in A 2 M 3 (SO 4) 4 (A = Rb, Cs; M = Co, Ni) analogues

Diana Nekrasova, Olivier Mentré, Oleg Siidra, Natacha Henry, Marie Colmont

Multiple dimensionalities in $A_2M_3(SO_4)_4$ (A = Rb, Cs; M = Co, Ni) analogues†

Diana O. Nekrasova,[a,b] Olivier Mentré,[a] Oleg I. Siidra,[b,c] Natacha Henry[a] and Marie Colmont *[a]

New representatives of the $A_2M_3(SO_4)_4$ (A = Rb and Cs, M = Co, Ni) family were found, inspired by the discovery and characterization of itelmenite, a mineral of composition $Na_2CuMg_2(SO_4)_4$. Four new compounds were obtained by high-temperature solid-state reactions in air. All new compounds were structurally characterized by single-crystal and powder X-ray diffraction. $Rb_2Ni_3(SO_4)_4$ and $Rb_2Co_3(SO_4)_4$ crystallize in the monoclinic space group $P2_1/c$, $Cs_2Ni_3(SO_4)_4$ in $P2_1/n$ whereas $Rb_2Co_3(SO_4)_4$ crystallizes in the orthorhombic space group $P2_12_12_1$. In order to determine the temperature of crystallization of the new phases DTA and TG were performed for the mixtures of the precursors. Several synthesis strategies were tested and discussed. The investigation of the reactivity upon heating highlights the stability of the precursors before they collapse, explaining the difficulties to get pure powder samples.

Introduction

In the last few decades, anhydrous alkali transition metal sulphates have received great attention. New materials have been developed, mainly inspired by minerals, for applications in the field of rechargeable batteries or magnetic materials. Due to this, a particular effort was made to investigate transition metal sulfates with light alkali metals like Li, Na and K in rare cases. As an example, the mineral-inspired eldfellite-type $NaFe(SO_4)_2$ [1] phase has been recently proposed as a low-cost cathode in a rechargeable Na-ion battery demonstrating about 80 mA h g^{-1} reversible capacity with a discharge voltage of 3.0 V *vs.* Na^+/Na for a relatively long life.[2] Other anhydrous compounds, *e.g.* $A_2M(SO_4)_2$,[3–5] $M_2(SO_4)_3$,[14,15] $A_2M(SO_4)_2$,[3,6] $AMSO_4(F, OH)$,[7,8] $A_2M_2(SO_4)_3$,[9] $A_2M_3O(SO_4)_3$ [10–12] and $A_2M_3(SO_4)_4$ [13,14] were structurally characterized and tested, not only as potential cathode materials, but also studied from the viewpoint of magnetic properties.[12,15,16] Nevertheless, to date the study of phases with heavier alkali metals, namely Rb and Cs remains scarce. To the best of our knowledge, $A_2M_2(SO_4)_3$ (A = Rb and K; M = Co, Ni, Cu, Fe or Mn)[9,17–21] and $A_2M(SO_4)_2$ (A = Rb or Cs and M = Cr, Fe, Co or Cu)[22,23] have been reported. The synthesis of such types of materials is subtle, strongly related to the particular mineral forming environments in nature. Natural anhydrous sulphates (mainly with copper) and alkali metals are formed as a result of high-temperature exhalative processes on volcanic fumaroles. At the moment, the natural growth conditions of sodium and potassium sulphate transition metal minerals are better known than those with rubidium or cesium. One of the striking examples of volcanoes rich in new mineral species is Tolbachik volcano, Kamchatka peninsula, Russia.[11,24] The mineral itelmenite[25] was first discovered there. Later, mimicking the natural process of mineral growth, the synthetic Mg, Zn-analogue was synthesized.[14] This mineral with its corresponding synthesis conditions and $K_2Cu_3(SO_4)_4$ [26] with the same formula type as the structures in this paper and that published in 2020 served as a prototype for the creation of a new family of compounds with a general formula $A_2M_3(SO_4)_4$ where A = alkali metal and M = transition metal, (A = Rb, Cs and M = Co, Ni).

In this paper we present the results of the synthesis and study of the four new compounds $Cs_2Ni_3(SO_4)_4$ (1), $Cs_2Co_3(SO_4)_4$ (2), $Rb_2Ni_3(SO_4)_4$ (3) and $Rb_2Co_3(SO_4)_4$ (4). The precursor mixtures were characterized using high temperature X-ray diffraction and thermal analysis to reveal the crystallization temperatures.

Experimental section

Synthesis of $Cs_2M_3(SO_4)_4$, M = Co and Ni

Crystals of $Cs_2Co_3(SO_4)_4$ and $Cs_2Ni_3(SO_4)_4$ were obtained by solid-state reactions in air using a stoichiometric ratio of

[a]*Unité de Catalyse et Chimie du Solide (UCCS), UMR 8181, 59655 Villeneuve d'ASCQ, France. E-mail: marie.colmont@centralelille.fr*
[b]*Department of Crystallography, St. Petersburg State University, University Embankment 7/9, 199034 St. Petersburg, Russia*
[c]*Kola Science Center, Russian Academy of Sciences, Apatity, Murmansk Region, 184200, Russia*

†Electronic supplementary information (ESI) available: Atom coordinates, bond-valence sums, thermal displacement parameters and selected interatomic distances for all crystal structures. CCDC 2110622–2110625. For ESI and crystallographic data in CIF or other electronic format see DOI: **https://doi.org/10.1039/d1dt04202e**

Cs_2SO_4, and MSO_4, M = Co and Ni (dehydrated at 400 °C during 12 hours). After grinding, the mixture was loaded into a gold crucible and heated to 600 °C for 3 hours and then cooled to 25 °C for 12 hours for the cobalt phase and to 700 °C for 10 hours and further slowly cooled to room temperature for 99 hours for the nickel one. The products consisted of prismatic purple crystals of the new $Cs_2Co_3(SO_4)_4$ compound in the $CoSO_4$ rich matrix for the cobalt sample and yellow irregularly shaped crystals of $Cs_2Ni_3(SO_4)_4$ with large amounts of unreacted Cs_2SO_4 for the nickel one. In both cases, other unknown impurities were registered by powder X-ray diffraction.

Synthesis of $Rb_2M_3(SO_4)_4$ (M = Ni, Co)

Crystals of $Rb_2M_3(SO_4)_4$ (M = Ni, Co) were obtained using Rb_2SO_4 and MSO_4 (M = Ni, Co) (dehydrated at 400 °C during night) reagents in a stoichiometric ratio. The mixtures of the precursors were ground, pressed into pellets (*ca.* 5 × 3 mm) and loaded into a quartz ampoule (*ca.* 8 × 0.8 mm) which was evacuated and sealed at an approximate pressure of 10^{-2} mbar. The quarts ampoules were placed into the furnace and heated at 750 °C for 18 hours for $Rb_2Ni_3(SO_4)_4$ and 34 hours for $Rb_2Co_3(SO_4)_4$ and then slowly cooled to room temperature for 99 hours. The final products consisted of yellow crystals of $Rb_2Ni_3(SO_4)_4$, $Rb_2Ni_2(SO_4)_3$ [27] and unreacted $NiSO_4$ and Rb_2SO_4 and violet crystals of $Rb_2Co_3(SO_4)_4$, $Rb_2Co_2(SO_4)_3$ [28] and $Co(SO_4)$.

Attempts to prepare the single-phase materials

Several trials to obtain polycrystalline samples were performed with stoichiometric amounts of $(Rb/Cs)_2SO_4$ and MSO_4 (M = Ni, Co) (also dehydrated at 400 °C for 12 hours). The main results are summarized in Table 1 and will be discussed later in the text.

Single-crystal X-ray analysis

Selected single crystals were mounted on thin glass fibers for X-ray diffraction (XRD) analysis using a Bruker APEX II DUO X-ray diffractometer equipped with a microfocus X-ray tube with MoKα radiation for $Cs_2Ni_3(SO_4)_4$, $Rb_2M_3(SO_4)_4$ (M = Ni and Co) and using a Bruker X8 diffractometer (Ag Kα radiation) for $Cs_2Co_3(SO_4)_4$. The data were integrated and corrected for absorption using a multi-scan type model implemented in the Bruker programs APEX3.[29] More than a hemisphere of X-ray diffraction data was collected for each crystal. The crystal structures of the new compounds were solved by direct methods and refined using the SHELXL program implemented in the WinGX[30] program package. Main crystallographic information is summarized in Table 2. Atom coordinates, bond-valence sums, thermal displacement parameters and selected interatomic distances for all crystal structures are provided in the ESI (Tables S1–S6†). The crystal structure of all compounds is shown in Fig. S1† with ADPs. CCDC numbers 2110625, 2110624, 2110623, and 2110622 contain the supplementary crystallographic data concerning new structures of this paper.†

Powder X-ray diffraction (XRD) analysis

Routine XRD analysis was performed at room temperature in the angular range of 2θ 5–60° with a scan step width of 0.02° and a scan rate of 0.5 s per step using a D8 Advance Bruker diffractometer (CuKα radiation, λ = 1.5405 Å). The XRD-patterns were analyzed using the DIFFRAC.EVA V4.0 software (Bruker).

High temperature X-ray diffraction (HTXRD) was performed using a Bruker D8 Advance associated with an Anton Paar XRK900 chamber and a 1D LynxEye detector using CuKα radiation. Data were collected from 10 to 60° at 2θ and upon heating in the temperature range from 20 to 550 °C (below plausible melting points).

Thermal analysis

TGA–DTA analysis was performed using a TGA 92-1600 SETARAM analyzer from RT to 1000° with a rate of 10° min^{-1} upon heating and under air.

Results and discussion

Structure of $Cs_2Ni_3(SO_4)_4$ (1)

Compound **1** crystallizes in the centrosymmetric space group $P2_1/n$ with unit-cell parameters a = 5.410(5), b = 18.444(16), c =

Table 1 Summary of the different syntheses attempted to prepare the title compounds and the obtained phases

Formula	T (°C)	Heating time (h)	Duration (h)	Cooling time (h)	PXRD analysis
$Cs_2Ni_3(SO_4)_4$	700	7	10	96 to 500 °C and 5 to 25 °C	$Cs_2Ni_3(SO_4)_4$, Cs_2SO_4.
	600	7	2	10 to 100 °C	$Cs_2Ni_3(SO_4)_4$, Cs_2SO_4, $NiSO_4$
$Cs_2Co_3(SO_4)_4$	600	7	3	12 to 100 °C	$Cs_2Co_3(SO_4)_4$, $Cs_2Co_2(SO_4)_3$, $CoSO_4$
	560	7	3	Quenched	$Cs_2Co_3(SO_4)_4$, $Cs_2Co_2(SO_4)_3$
	530	7	2	60 to 100 °C	$Cs_2Co_3(SO_4)_4$, $Cs_2Co_2(SO_4)_3$
$Rb_2Ni_3(SO_4)_4$	750	7	18	96 to 500 °C	$Rb_2Ni_3(SO_4)_4$, Rb_2SO_4
	600	7	1.5	10 to 100 °C	$Rb_2Ni_3(SO_4)_4$, $Rb_2Ni_2(SO_4)_3$
	600	7	24	10 to 100 °C	$Rb_2Ni_2(SO_4)_3$, $NiSO_4$
	600	7	24	70 to 500 °C and 10 to 25 °C	$Rb_2Ni_3(SO_4)_4$, $Rb_2Ni_2(SO_4)_3$, $NiSO_4$
	600	7	6	Furnace off	$Rb_2Ni_3(SO_4)_4$, $Rb_2Ni_2(SO_4)_3$, $NiSO_4$
$Rb_2Co_3(SO_4)_4$	750	7	34	40 to 200 °C	$Rb_2Co_3(SO_4)_4$, $Rb_2Co_2(SO_4)_3$
	600	7	1.5	10 to 100 °C	$Rb_2Co_3(SO_4)_4$, $Rb_2Co_2(SO_4)_3$, $CoSO_4$
	600	7	24	10 to 100 °C	$Rb_2Co_3(SO_4)_4$, $Rb_2Co_2(SO_4)_3$, $CoSO_4$

Table 2 Crystallographic and structure refinement data for $A_2M_3(SO_4)_4$ (A = Cs, Rb; M = Ni, Co)

$A_2M_3(SO_4)_4$	$Cs_2Ni_3(SO_4)_4$	$Cs_2Co_3(SO_4)_4$	$Rb_2Ni_3(SO_4)_4$	$Rb_2Co_3(SO_4)_4$
Empirical formula	$Ni_3Cs_2O_{16}S_4$	$Co_3Cs_2O_{16}S_4$	$Ni_3O_{16}Rb_2S_4$	$Co_3O_{16}Rb_2S_4$
Formula weight	826.19	826.85	731.31	731.97
Temperature/K	296.15	296.15	296.15	296.15
Crystal system	Monoclinic	Orthorhombic	Monoclinic	Monoclinic
Space group	$P2_1/n$	$P2_12_12_1$	$P2_1/c$	$P2_1/c$
a/Å	5.399(2)	9.0576(8)	9.2661(15)	9.3678(4)
b/Å	18.340(7)	9.9193(7)	8.5703(13)	8.6386(3)
c/Å	7.596(3)	15.8622(13)	9.2865(15)	9.3763(6)
α/°	90	90	90	90
β/°	104.581(8)	90	119.009(3)	119.1660(10)
γ/°	90	90	90	90
Volume/Å^3	727.9(5)	1425.1(2)	644.95(18)	662.57(6)
Z	2	4	2	2
$\rho_{calc.}$/g cm^{-3}	3.769	3.854	3.766	3.669
μ/mm^{-1}	9.429	4.791	12.577	11.736
F(000)	772.0	1532.0	700.0	694.0
Crystal size/mm^3	0.08 × 0.06 × 0.05	0.1 × 0.08 × 0.04	0.12 × 0.09 × 0.06	0.11 × 0.07 × 0.05
Radiation	MoKα (λ = 0.71073)	AgKα (λ = 0.56086)	MoKα (λ = 0.71073)	MoKα (λ = 0.71073)
2Θ range for data collection/°	5.97 to 52.984	4.052 to 55.998	5.026 to 71.692	4.98 to 94.64
Index ranges	$-6 \le h \le 6$, $-22 \le k \le 22$, $-9 \le l \le 9$	$-15 \le h \le 15$, $-15 \le k \le 16$, $-26 \le l \le 26$	$-10 \le h \le 15$, $-14 \le k \le 14$, $-15 \le l \le 12$	$-16 \le h \le 18$, $-17 \le k \le 16$, $-17 \le l \le 15$
Reflections collected	8039	62 948	9305	20 415
Independent reflections	1498 [R_{int} = 0.0623, R_{sigma} = 0.0509]	7020 [R_{int} = 0.0674, R_{sigma} = 0.0465]	2939 [R_{int} = 0.0378, R_{sigma} = 0.0505]	5064 [R_{int} = 0.0516, R_{sigma} = 0.0546]
Data/restraints/parameters	1498/0/116	7020/0/226	2939/0/116	5064/0/115
Goodness-of-fit on F^2	1.047	1.072	1.047	1.013
Final R indexes [$I \ge 2\sigma(I)$]	R_1 = 0.0408, wR_2 = 0.0863	R_1 = 0.0328, wR_2 = 0.0536	R_1 = 0.0322, wR_2 = 0.0576	R_1 = 0.0365, wR_2 = 0.0655
Final R indexes [all data]	R_1 = 0.0613, wR_2 = 0.0942	R_1 = 0.0483, wR_2 = 0.0596	R_1 = 0.0544, wR_2 = 0.0626	R_1 = 0.0714, wR_2 = 0.0742
Largest diff. peak/hole/e Å^{-3}	0.85/−0.84	1.07/−1.82	1.07/−0.94	1.10/−2.14
Flack parameter		−0.039(12)		

7.618(7) and β = 104.56(3)°. It shows a layered crystal structure with sheets containing two independent octahedral Ni^{2+} crystallographic sites. The layers contain $_\infty$[Ni1–Ni1–Ni2–Ni2] chains running along the c-axis. Two $Ni2O_6$ octahedra form dimers *via* sharing of the common edge. The connection between adjacent chains by Ni1–O–Ni2 bridges builds thus 2D sheets (see Fig. 1a) in the *ac* plane. $Ni1O_6$ is quite regular with an average ⟨Ni–O⟩ bond length of around 2.08 Å, whereas the $Ni2O_6$ octahedra (similar ⟨Ni–O⟩ = 2.08 Å) are distorted due to Ni off-centering induced by their multiple connectivity types. It shows *cis* O–Ni–O angles between 67° and 101° (Fig. 2a). The Ni–Ni distance values (between 3.2635(18) and 3.6220(15) Å, see Fig. 1a) offer possible exchanges through Ni–O–Ni super-exchange interactions. The two independent SO_4 tetrahedra show standard S^{6+}–O bond distances varying between 1.4387(57) and 1.5214(57) Å and O–S^{6+}–O bond angles in the range 102.2(2)–112.5(2)°. The edge-sharing of $S1O_4$ with $Ni2O_6$ is, to the best of our knowledge, new (see Fig. 1b). Only a few examples of similar configurations are referenced so far for other transition metals such as Cu.[26,31] The interlayer distance is about 2.85(1) Å.

Cesium atoms are located in the interlayer space and counter-balance the layer charges. They are surrounded by 8 oxygens forming irregular polyhedra, where the Cs–O bond lengths are in the range of 3.043(5)–3.449(5) Å.

Structure of $Cs_2Co_3(SO_4)_4$ (2)

Compound **2** crystallizes in an orthorhombic unit cell with unit cell parameters a = 9.0576(8) Å, b = 9.9193(7) Å and c = 15.8622(13) Å (non-centrosymmetric S.G. $P2_12_12_1$). Its three-dimensional structure contains two symmetrically independent Cs^+, three Co^{2+}, and four S^{6+} cations. The atoms Co1 and Co3 have distorted octahedral coordination with the bond lengths between 2.044(4) and 2.200(4) Å for Co1 and from 1.999(4) to 2.240(3) Å for Co3 (Fig. 3a). Co2 forms a CoO_5 square pyramid with the bond lengths in the range 1.995(3)–2.109(3) Å. Such an octahedral distortion can be interpreted on the basis of the Co^{2+} Jahn–Teller effect, in comparison with the more regular Ni^{2+} coordination in the compound **2** Ni-analogue. From the viewpoint of Co–O–Co connectivity, $Co(2)O_5$ and $Co(3)O_6$ polyhedra are connected together through corner sharing (O10) into $[Co_2O_{10}]^{16-}$ dimers (Fig. 3a and 4a) leaving isolated $Co1O_6$. The SO_4 tetrahedra are regular with S–O bond distances between 1.431(4) and 1.482(3) Å. The SO_4 tetrahedra are linked with cobalt polyhedra through common oxygen atoms for S1, S3 and S4 and through edge sharing with Co3 for S2, forming a compact 3D framework (Fig. 4b and c). Cs atoms are located in the voids. Cs^+ cations are surrounded by ten O^{2-} anions with the Cs–O bond lengths in the range of 3.027(4)–3.482(5) Å for Cs1 and 3.058(4)–3.416(4) Å for Cs2

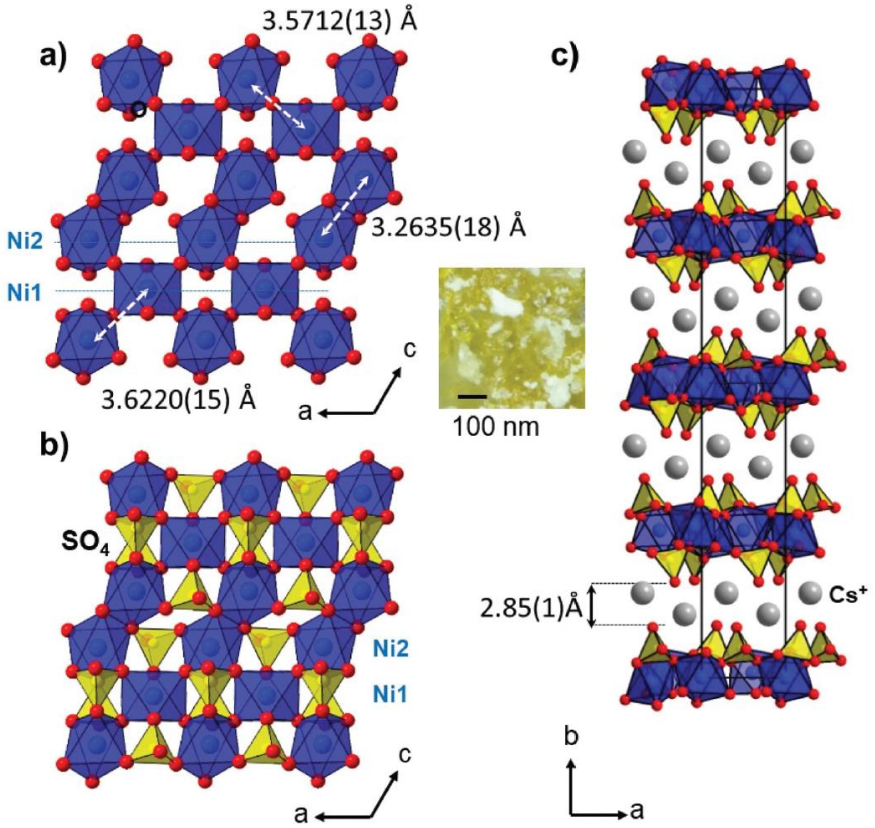

Fig. 1 2D blocks in **1** projected on the *ac* plane with (a) NiO_6 octahedra (blue) connected to (b) SO_4 tetrahedra (yellow) and (c) general projection of the crystal structure of **2** along the *c*-axis, showing the stacking and the interstitial Cs^+ cations (grey balls). The photo in the inset shows the color and shape of crystals.

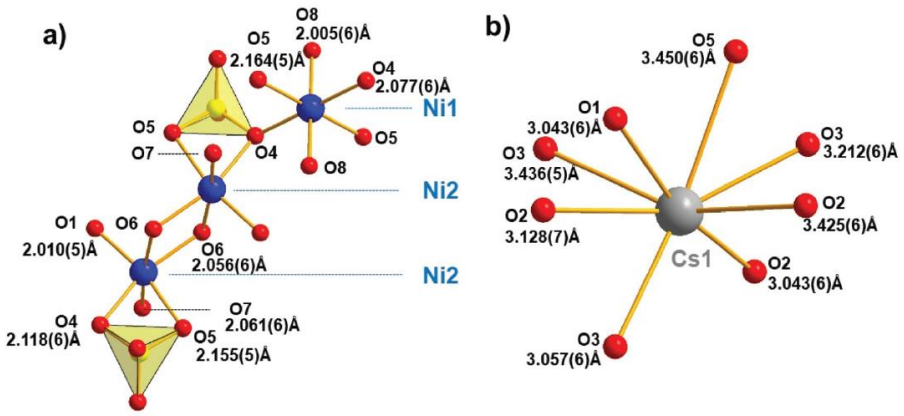

Fig. 2 Coordination of (a) Ni^{2+} and (b) Cs^+ cations in the crystal structure of **1**. Only sulphates sharing edges with NiO_6 octahedra are shown. The distances are given in Angströms.

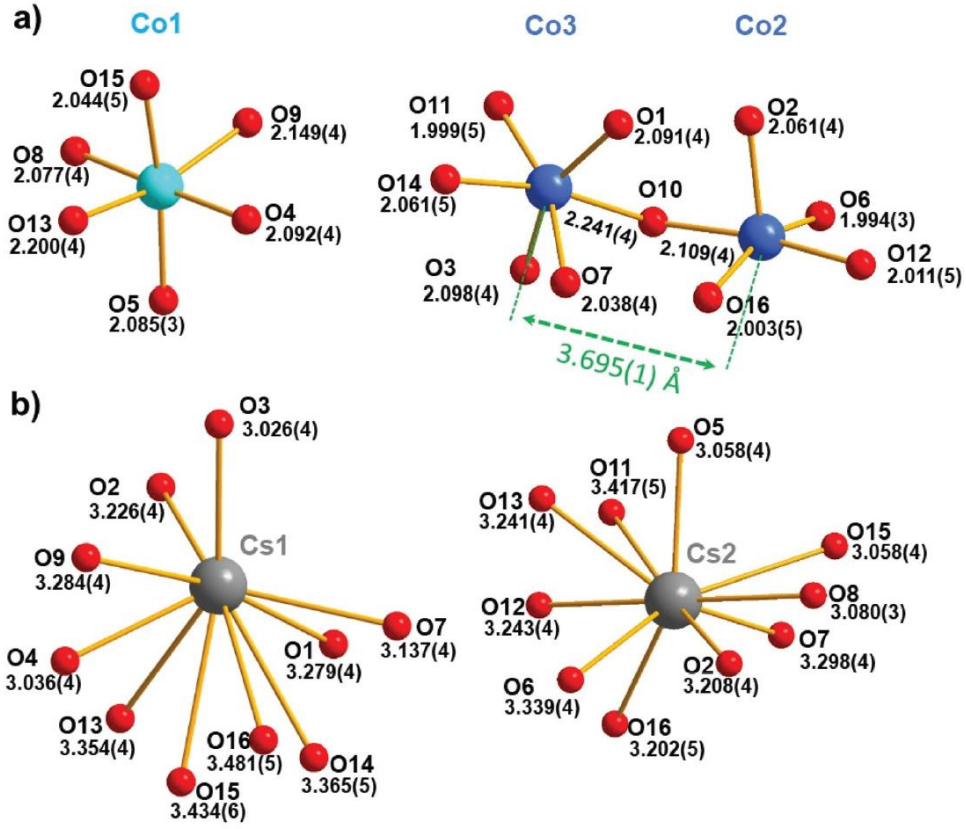

Fig. 3 Coordination environments of Co (a) and Cs (b) atoms in the crystal structure of **2**. The distances are given in Angströms.

(Fig. 3b). The crystal structure is shown in Fig. 4d. It is remarkable that although they have a similar chemical formula, compounds **1** and **2** adopt different crystal structures and dimensionalities. At the first glance, the specific coordination of the three CoO_n polyhedra drives the 3D connectivity and, once again, maybe be originally influenced by the significant JT effect for Co^{2+} in this complex crystal structure, when associated with large compressive Cs^+ alkali.

$Rb_2M_3(SO_4)_4$, M = Ni (3) and Co (4)

In contrast to what is observed for A = Cs^+ (r = 1.74 Å for 8 neighbors), smaller Rb^+ cations (r = 1.61 Å for 8 neighbors) stabilize isotypic crystal structures for **3** and **4** in a monoclinic symmetry. The unit-cell parameters are a = 9.2661(15) Å, b = 8.5703(13) Å, c = 9.2865(15) Å, and β = 119.01 (1)° for Ni and a = 9.3678(4) Å, b = 8.6386(3) Å, c = 9.3763(6) Å, and β = 119.17 (1)° for Co with the space group $P2_1/c$. The two structures contain one independent crystallographic position for Rb^+, and two for S^{6+} and M^{2+} (M = Ni and Co). The specific environments of the cations are presented in Fig. 5. The rubidium atoms are coordinated by eight O^{2-} with Rb–O bond lengths in the range of 2.7751(18)–3.1300(18) Å in the crystal structure of **3** and of 2.8072(13)–3.1426(14) Å in the crystal structure of **4**. The atoms Co1 and Co2 have an octahedral coordination with bond lengths ranging from 2.0112(13) to 2.1874(13) Å for Co1 and from 1.9990(13) to 2.3938(13) Å for Co2. The Ni–O bond lengths vary from 1.9856(17) to 2.1481(17) Å for Ni1 and from 1.9759(17) to 2.3770(17) Å for Ni2. The MO_6 octahedra are connected together through corner sharing, building isolated $[M_3O_{16}]^{26-}$ trimers (see Fig. 6a).

Sulphates, where the average value of the distance ⟨S–O⟩ is 1.472 Å for **3** and 1.471 for (**4**), are pulling trimers together through oxygen sharing, building a 3D framework with empty 1D channels running along the c-axis and hosting Rb^+ cations (see Fig. 6b and c).

Comparing the different structural types, the nature of alkali and transition metals necessarily affects the crystal structure and its complexity. This latter parameter can be quantified using the calculation developed by Krivovichev[32] and based on the Shannon information theory[33] and also based on the unit cell and its number and the nature of atoms. The total structural information value ($I_{G,total}$ (bits per unit-cell)) of all

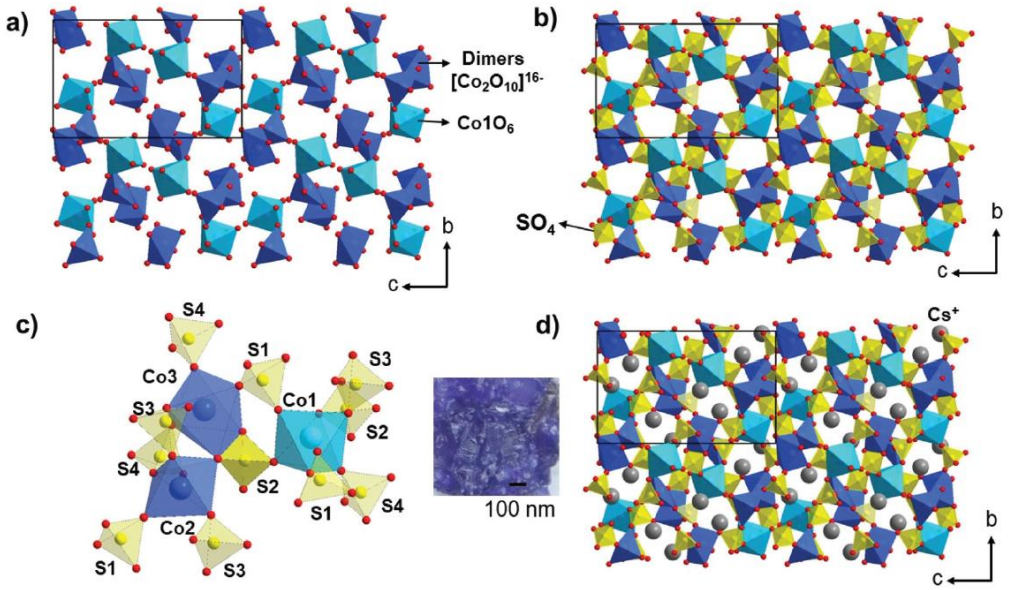

Fig. 4 (a) Association between Co_2O_{10} dimers (dark blue) and CoO_6 octahedra (turquoise blue) in the *bc* plane and (b) connected to SO_4 tetrahedra (yellow). (c) The connectivity between the different polyhedra is detailed and (d) the whole structure with the Cs^+ cations (in grey) is shown along the *a*-axis.

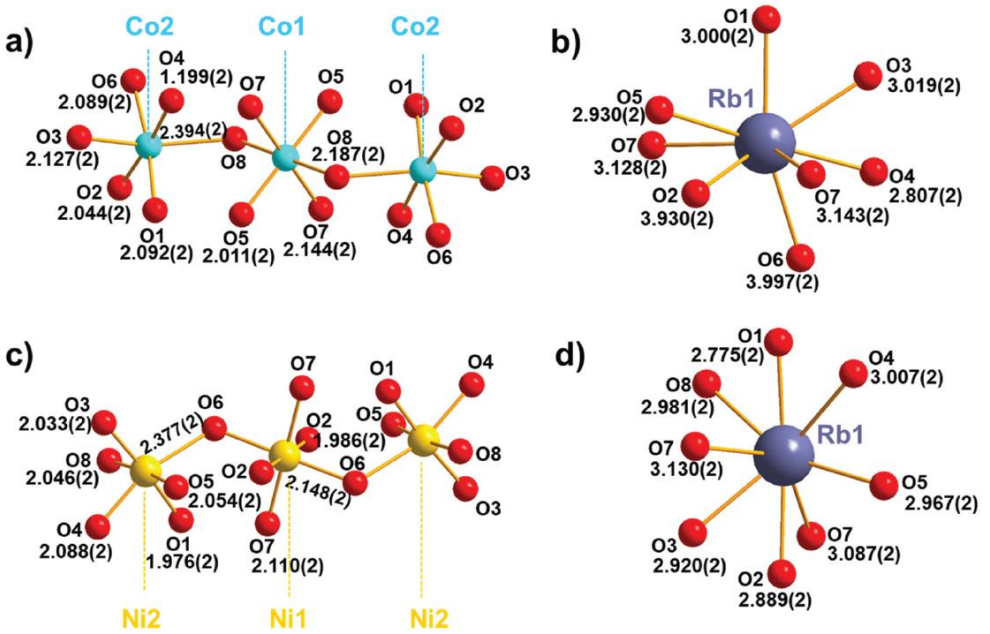

Fig. 5 MO_6 octahedra sharing corners giving M_3O_{16} trimers (a) in **4** (*M* = Co) and (c) in **3** (*M* = Ni) and Rb^+ environments (b) in **4** and (d) in **3**. The cation–oxygen bond distances are given in Angströms.

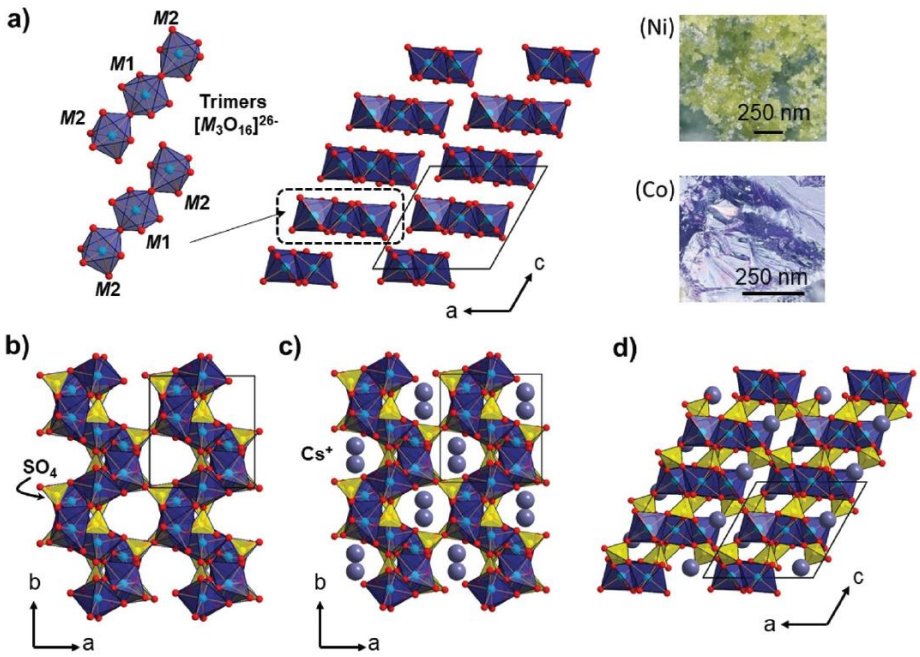

Fig. 6 (a) M_3O_{16} trimers (in blue) and their association in the *ac* plane, (b) association of SO_4 tetrahedra (in yellow) to the trimers, building 1D cavities running along the *c*-axis; these cavities are hosting Cs^+ cations (in grey) and the final crystal structures are shown along the (c) *c*- and (d) *b*-axis. In the inset, the photos show the crystal shapes of Co and Ni compounds.

structures was calculated using ToposPro.[34] Compounds **1**, **3** and **4** show similar structural complexity with $I_{G,total}$ = 184.193 bit per cell. Concerning compound **2**, $I_{G,total}$ is equal to 464.386 bit per cell which is higher than those of the other three phases. Of course, it is reminiscent of the largely reduced cell volume, almost double, compared to other crystal types. Again, there is no obvious relationship between the calculated complexity and the nature of the alkali. This level of complexity is called "intermediate" as mentioned by Krivovichev in ref. 32 representing around 23% of inorganic structures.

The presence of dimers and trimers appears to be interesting as it may give rise to interesting magnetic coupling as suggested by the Goodenough–Kanamori rules. Consequently, strong attention has been paid to the obtaining of single-phase polycrystalline materials.

Phases reactivity

In order to obtain polycrystalline samples, the reactivity of the precursors was analyzed using thermogravimetric analysis and HTXRD. HTXRD studies were performed up to 550 °C to avoid melting of the sample in the sample holder.

Phases 1 and 2. A mixture of Cs_2SO_4 and $NiSO_4$/$CoSO_4$ (just dehydrated) in a 1 : 3 ratio was prepared, and finely ground and TGA and DTG analyses were performed using a thermoanalyzer TGA 92 SETARAM working under an air atmosphere. The samples were heated at 10 °C min^{-1} from 30 °C up to 1000 °C. For *M* = Ni, the TGA curve observed in Fig. 7a evidenced several thermal processes below 150 °C which is consistent with the loss of water molecules of the precursors as already detailed in ref. 35. Keeping in mind the preliminary dehydration stage and short time of contact with air, it highlights the problematic extreme reactivity of the sulphate precursors to moisture through the example of $CsNi(SO_4)_2{\cdot}6H_2O$ being already evidenced under ambient conditions. In agreement with the HTXRD results (see Fig. 7b), the removal of water molecules occurs between 50 and 150 °C. A first uncomplete reaction is observed by XRD at 350 °C corresponding to the growth of $Cs_2Ni_3(SO_4)_4$ accompanied by residual Cs_2SO_4 and $NiSO_4$ (Fig. 7c). At 700 °C, a weight loss is observed in TGA analysis corresponding to the decomposition through the removal of sulphate molecules. Thus, sulphate decomposition occurs with the formation of SO_3 which quickly decomposes to release $SO_2 + \frac{1}{2}O_2$.[35]

For compound **2**, TGA and HTXRD results are shown in Fig. 7d–f. A general behaviour similar to the one previously discussed was observed: it corresponds to the dehydration of the precursors occurring up to 330 °C. The peak at 531 °C corresponds to the crystallization and formation of $Cs_2Co_3(SO_4)_4$ and $Cs_2Co_2(SO_4)_3$. The endothermic peak at 850 °C belongs to the

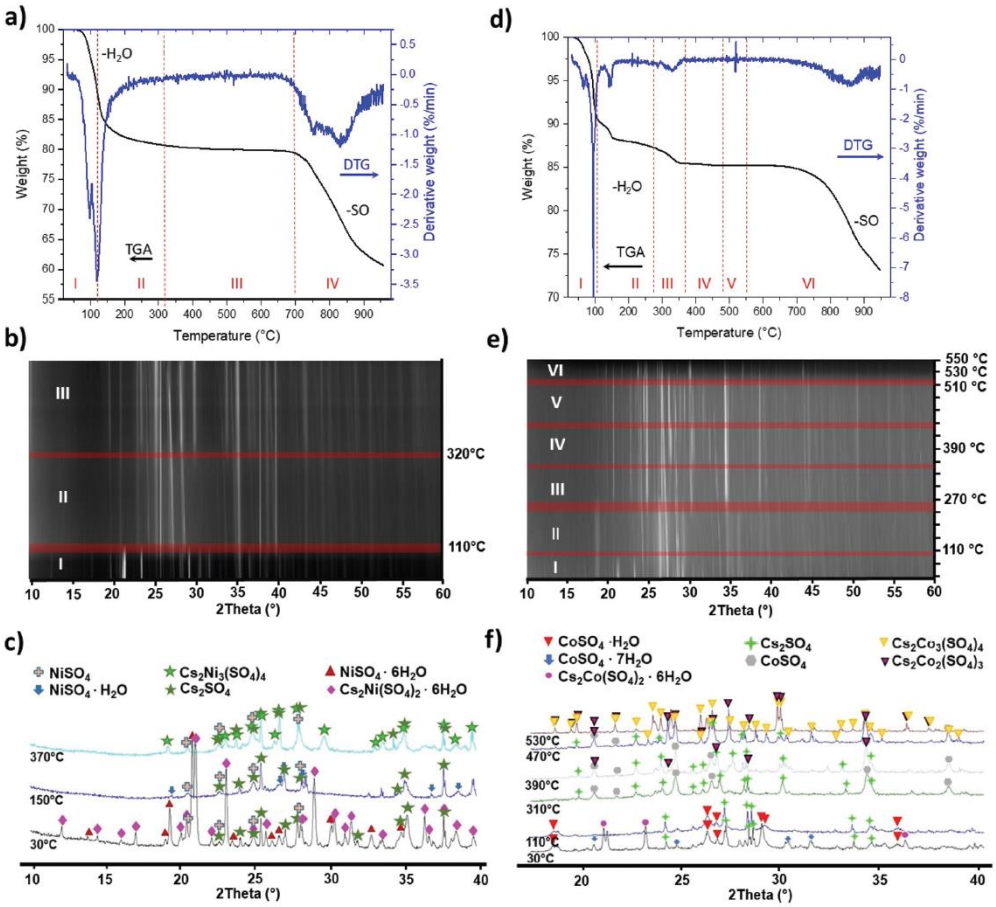

Fig. 7 TGA–DTA curves from 30 °C to 1000 °C for the mixture of precursors for **1** (a) Cs_2SO_4 and $NiSO_4$ and for **2** (d) Cs_2SO_4 and $CoSO_4$ in a 1 : 3 ratio; an HTXRD study explained their transitions in the case of (b) **1** and (e) **2**. For **1**, step I–II correspond to the dehydration process, step III–IV to the formation of $Cs_2Ni_3(SO_4)_4$ and step V to the collapse of the sample by sulphate removal (a and b). For **2**, step I–II correspond to the dehydration process, where the sixth water molecule is discharged, step III to the lost seventh molecule, IV–V – formation of $Cs_2Co_3(SO_4)_4$ and $Cs_2Co_2(SO_4)_3$, and VI – the decomposition process (HTXRD from 30 °C to 350 °C with step 40 °C; 350–550 °C – step 20 °C). Phase identification on some selected patterns registered at different temperatures on mixtures of precursors for (c) **1** and (f) **2**.

decomposition process of the sulphate compounds. Details of the pattern identification at all stages are given in Fig. 7f for **2**.

Several trials were performed at temperatures of synthesis chosen on the plateau of the TGA: 600 °C and 700 °C for **1** and 530 °C, 560 °C and 600 °C for **2** and for several durations, even long ones. All of them led to the synthesis of the targeted phase but systematically resulted in a significant amount of unreacted phase impurities as detailed in Table 1. This is a proof of the high stability upon heating of the precursors (Cs_2SO_4 and $NiSO_4$) that finally collapse with the compounds before their pure obtention.

Phases 3 and 4. Then, a similar procedure was used to attempt the synthesis of pure powder samples of **3** and **4** and again, the results highlight the dehydration of the precursors followed by the formation of $Rb_2M_2(SO_4)_3$ and $Rb_2M_3(SO_4)_4$ (M = Ni and Co). At a high temperature (790 °C for Ni and 820 °C for Co) (step VII) – the decomposition process starts to form the simple NiO and CoO oxides and release SO_2. The detailed XRD patterns are presented in Fig. 8c and f. Here again, $NiSO_4$ and $CoSO_4$ are stable up to a high temperature, making impossible the obtention of pure powder samples through this way and independent of heating times.

At the end, changing the synthesis conditions (temperature in the accurate zone of heating, duration or cooling) never allowed us to obtain the pure phase. Also, in the cases of **2** and **4** there is a demixing of a part of $A_2M_3(SO_4)_4$ leading to the formation of the required $A_2M_3(SO_4)_4$ with the sub products $A_2M_2(SO_4)_3$ + MSO_4. Despite many attempts, the synthesis of the pure powder samples systematically failed due to thermodynamical reasons. It is obvious that the non-total dehydration

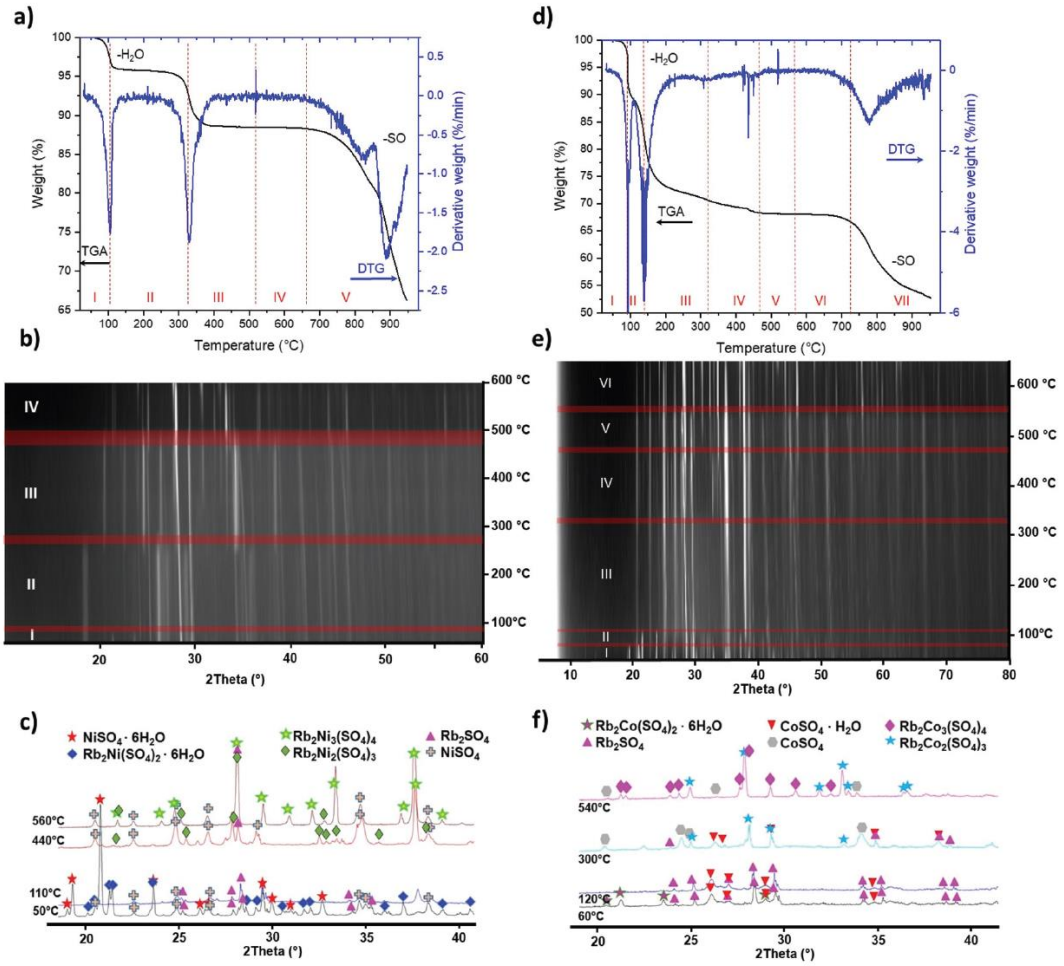

Fig. 8 TGA–DTA curves from 30 °C to 1000 °C for the mixture of (a) Rb_2SO_4 and $NiSO_4$ and (c) Rb_2SO_4 and $CoSO_4$ in a 1 : 3 ratio; an HTXRD study explained their transitions in the case of (b) Ni and (d) Co. For the Ni-sample, I–III steps correspond to the dehydration of $NiSO_4{\cdot}6H_2O$ as a three-stage process, step V–VI – formation of $Rb_2Ni_2(SO_4)_3$ and $Rb_2Ni_3(SO_4)_4$, and step VII – decomposition; for the Co-sample, I–II – hydrated precursors, III – anhydrous precursors and formation of $Rb_2Co_2(SO_4)_3$, IV – formation of $Rb_2Co_3(SO_4)_4$, and V – decomposition. Phase identification on some selected patterns registered at different temperatures on mixtures of precursors for (c) **3** and (f) **4**.

of the precursors is a problem concerning the strict preservation of the stoichiometry. To avoid this, several trials were performed, with increasing a small percent (5%) the amount of cesium/rubidium sulfate. Nevertheless, the results were always identical. On the other hand, some trials will focus on other types of syntheses, such as inducing other media and using other thermodynamical processes like hydrothermal synthesis and chemical vapor transport. Indeed, these two processes will induce some pressure, usually observed in nature through generation of exhausting hot gases depending on many parameters like temperature, nature of gases, humidity *etc*. Also, the synthesis conditions are sometimes exotic and difficult to reproduce in a laboratory.[36]

Conclusion

In this paper, four new cesium/rubidium transition metal (nickel and cobalt) sulphates were prepared and their crystal structures solved. $Rb_2Co_3(SO_4)_4$ and $Rb_2Ni_3(SO_4)_4$ show 3D frameworks with 1D tunnels hosting Rb^+ cations. $Cs_2Co_3(SO_4)_4$ and $Cs_2Ni_3(SO_4)_4$ indeed crystallize in different forms; the cobalt analog is 3D whereas the nickel one is 2D with parallel layers surrounded by isolated Cs^+ cations. The calculation of their complexity shows that all the compounds presented here are in a medium range of complexity, as 23% of inorganic materials. The connectivity between the cobalt/nickel polyhedra offers promising magnetic properties but at the moment,

the preparation of the targeted phases did not give single phase materials, using solid state synthesis routes. The reactivity investigation shows the impossibility to obtain pure powder samples through this route due to the high stability of the precursors upon heating and the collapse of the targeted phase before its full obtention. Further works will focus on the use of alternative processes such as coprecipitation, hydrothermal synthesis or chemical vapor transport (CVT). Indeed, in nature, an autogenous pressure is usually observed and plays probably a key role in the crystal growth of minerals.

Conflicts of interest

There are no conflicts to declare.

Acknowledgements

This work was supported by the Embassy of France in Russia, the French Government, and managed by the Agency Campus France. The Fonds Européen de Développement Régional, CNRS, Région Nord Pas-de-Calais, and Ministère de l'Education Nationale de l'Enseignement Supérieur et de la Recherche are acknowledged for funding the X-ray diffractometers.

References

1 T. Balić-Žunic, A. Garavelli, P. Acquafredda, E. Leonardsen and S. P. Jakobsson, Eldfellite, $NaFe(SO_4)_2$, a new fumarolic mineral from Eldfell volcano, Iceland, *Mineral. Mag.*, 2009, **73**(1), 51–57, DOI: **10.1180/minmag.2009.073.1.51**.

2 P. Singh, K. Shiva, H. Celio and J. B. Goodenough, Eldfellite, $NaFe(SO_4)_2$: an intercalation cathode host for low-cost Na-ion batteries, *Energy Environ. Sci.*, 2015, **8**(10), 3000–3005, DOI: **10.1039/C5EE02274F**.

3 M. Reynaud, G. Rousse, J.-N. Chotard, J. Rodríguez-Carvajal and J.-M. Tarascon, Marinite $Li_2M(SO_4)_2$ (M = Co, Fe, Mn) and $Li_1Fe(SO_4)_2$: Model Compounds for Super-Super-Exchange Magnetic Interactions, *Inorg. Chem.*, 2013, **52**(18), 10456–10466, DOI: **10.1021/ic401280e**.

4 A. Manthiram and J. B. Goodenough, Lithium insertion into $Fe_2(SO_4)_3$ frameworks, *J. Power Sources*, 1989, **26**(3–4), 403–408, DOI: **10.1016/0378-7753(89)80153-3**.

5 J. Gaubicher, J. Angenaut, Y. Chabre, T. Le Mercier and M. Quarton, Lithium Electrochemical Intercalation/Deintercalation in Rhombohedral $V_2(SO_4)_3$, *Mol. Cryst. Liq. Cryst. Sci. Technol., Sect. A*, 1998, **311**(1), 45–50, DOI: **10.1080/10587259808042364**.

6 L. Lander, *et al.*, Unveiling the electrochemical mechanisms of $Li_2Fe(SO_4)_2$ polymorphs by neutron diffraction and density functional theory calculations, *Phys. Chem. Chem. Phys.*, 2016, **18**(21), 14509–14519, DOI: **10.1039/C6CP02175A**.

7 P. Barpanda, *et al.*, Structure and electrochemical properties of novel mixed $Li(Fe_{1-x}M_x)SO_4F$ (M = Co, Ni, Mn) phases fabricated by low temperature ionothermal synthesis, *J. Mater. Chem.*, 2010, **20**(9), 1659, DOI: **10.1039/b922063a**.

8 M. Reynaud, *et al.*, Synthesis and crystal chemistry of the $NaMSO_4F$ family (M = Mg, Fe, Co, Cu, Zn), *Solid State Sci.*, 2012, **14**(1), 15–20, DOI: **10.1016/j.solidstatesciences.2011.09.004**.

9 L. Lander, G. Rousse, D. Batuk, C. V. Colin, D. A. Dalla Corte and J.-M. Tarascon, Synthesis, Structure, and Electrochemical Properties of K-Based Sulfates $K_2M_2(SO_4)_3$ with M = Fe and Cu, *Inorg. Chem.*, 2017, **56**(4), 2013–2021, DOI: **10.1021/acs.inorgchem.6b02526**.

10 G. L. Starova, S. K. Filatov, V. S. Fundamensky and L. P. Vergasova, The crystal structure of fedotovite, $K_2Cu_3O(SO_4)_3$, *Mineral. Mag.*, 1991, **55**(381), 613–616, DOI: **10.1180/minmag.1991.055.381.14**.

11 O. I. Siidra, *et al.*, Copper oxosulphates from fumaroles of Tolbachik volcano: puninite, $Na_2Cu_3O(SO_4)_3$ – a new mineral species and structure refinements of kamchatkite and alumoklyuchevskite, *Eur. J. Mineral.*, 2017, **29**(3), 499–510, DOI: **10.1127/ejm/2017/0029-2619**.

12 D. O. Nekrasova, A. A. Tsirlin, M. Colmont, O. Siidra, H. Vezin and O. Mentré, Magnetic hexamers interacting in layers in the $(Na, K)_2Cu_3O(SO_4)_3$ minerals, *Phys. Rev. B*, 2020, **102**(18), 184405, DOI: **10.1103/PhysRevB.102.184405**.

13 J. Gao, X. Sha, X. Liu, L. Song and P. Zhao, Preparation, structure and properties of $Na_2Mn_3(SO_4)_4$: a new potential candidate with high voltage for Na-ion batteries, *J. Mater. Chem. A*, 2016, **4**(30), 11870–11877, DOI: **10.1039/C6TA02629J**.

14 D. O. Nekrasova, *et al.*, A fumarole in a one-pot: synthesis, crystal structure and properties of Zn- and Mg-analogs of itelmenite and a synthetic analog of glikinite, *Phys. Chem. Miner.*, 2021, **48**(1), 6, DOI: **10.1007/s00269-020-01132-4**.

15 L. Lander, G. Rousse, A. M. Abakumov, M. Sougrati, G. van Tendeloo and J.-M. Tarascon, Structural, electrochemical and magnetic properties of a novel $KFeSO_4F$ polymorph, *J. Mater. Chem. A*, 2015, **3**(39), 19754–19764, DOI: **10.1039/C5TA05548B**.

16 L. Lander, M. Reynaud, J. Rodríguez-Carvajal, J.-M. Tarascon and G. Rousse, Magnetic Structures of Orthorhombic $Li_2M(SO_4)_2$ (M = Co, Fe) and $Li_xFe(SO_4)_2$ (x = 1, 1.5) Phases, *Inorg. Chem.*, 2016, **55**(22), 11760–11769, DOI: **10.1021/acs.inorgchem.6b01844**.

17 G. Gattow and J. Zemann, Uber Doppelsulfate vom Langbeinit-Typ, $A_2^+B_2^{2+}(SO_4)_3$, *Z. Anorg. Allg. Chem.*, 1958, **293**(5–6), 233–240, DOI: **10.1002/zaac.19582930502**.

18 T. Hikita, H. Sekiguchi and T. Ikeda, Phase Transitions in New Langbeinite-Type Crystals, *J. Phys. Soc. Jpn.*, 1977, **43**(4), 1327–1331, DOI: **10.1143/JPSJ.43.1327**.

19 H. F. McMurdie, M. C. Morris, J. deGroot and H. E. Swanson, Crystallography of some double sulfates and chromates, *J. Res. Natl. Bur. Stand., Sect. A*, 1971, **75A**(5), 435, DOI: **10.6028/jres.075A.034**.